Colloids and Surfaces A 560 (2019) 189–197

Contents lists available at ScienceDirect

Colloids and Surfaces A

journal homepage: www.elsevier.com/locate/colsurfa

Effect of surfactant concentration on foam texture and flow characteristics in porous media

Li Binfei[a], Li Haifeng[a], Cao Aiqing[b], Wang Fei[c,*]

[a] School of Petroleum Engineering, China University of Petroleum (East China), Qingdao, 266580, Shandong, China
[b] School of Mechanical and Electrical Engineering, China University of Petroleum (East China), Qingdao, 266580, Shandong, China
[c] Geo-Energy Research Institute, Faculty of Electromechanical Engineering, Qingdao University of Science and Technology, Qingdao, 266061, Shandong, China

GRAPHICAL ABSTRACT

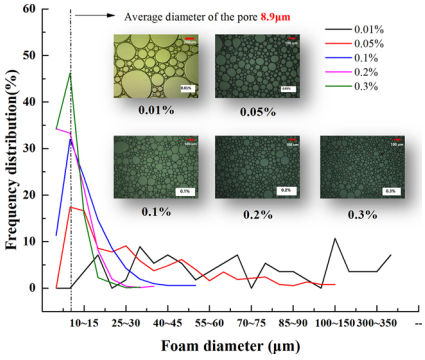

ARTICLE INFO

Keywords:
Surfactant concentration
Foam texture
Flow characteristics
Diameter matching degree
Gas saturation

ABSTRACT

Foam has been widely used for profile control, water plugging, and gas channeling control in enhanced oil recovery (EOR). Because of absorption, the surfactant concentration in foam decreases along the flow direction. In this study, the effects of surfactant concentration on the foam texture, foam seepage characteristics, and gas saturation were evaluated by core-flow experiments using a high-pressure visualization device. The results show that the surface tension of gas and liquid decreases, the flow resistance in core increases, and the foam takes a longer time to reach stability with the increase in concentration of foaming agent. The blocking capability of foam in porous media is closely related to foam texture. With the increase in surfactant concentration, the average diameter of bubbles in porous media decreases, and the bubbles are more uniform. Moreover, the diameter of bubbles is closer to the average pore diameter of core. Clearly, the diameter matching degree of the maximum distribution frequency of bubbles and the average pore diameter of core increase. Therefore, the blocking capability of foam becomes stronger. With the increase in surfactant concentration, the proportion of trapped gas in porous media increases, the gas saturation in core increases, and the flow resistance of foam increases. However, when the surfactant concentration reaches the critical value, the increasing amplitude of gas saturation decreases. Under an injected foam quality of 50%, the gas saturation is more than 80%. The research results can help to analyze the change along the channel of foam flow in formation and are of great significance to improve the effect of foam application.

* Corresponding author.
E-mail address: wangfeiupc@163.com (F. Wang).

https://doi.org/10.1016/j.colsurfa.2018.10.027
Received 15 May 2018; Received in revised form 9 August 2018; Accepted 8 October 2018
Available online 09 October 2018

1. Introduction

Aqueous foam is a dispersion of gas in continuous water stabilized by a surfactant. It has been widely used for profile control (the operation of plugging the high permeability layer from the injection well and adjusting the water injection profile of the water injection section), water plugging (the operation of plugging high permeability layer from oil well and reducing the water production of the well), and gas channeling control (the operation of decreasing the injected gas mobility and adjusting the level of infiltration layer suction profile) in enhanced oil recovery (EOR) processes [1–8]. Foam can sharply decrease the mobility of gas and improve the sweep efficiency of flooding fluid in the formation, thus enhancing oil recovery [9–18].

The ability of foam in decreasing gas mobility or increasing sweep efficiency is strongly related to the foam texture; it depends on gas/liquid ratio, flow rate, surfactant property, and concentration [19,20].

In a foam system, the addition of a surfactant to water can decrease the surface tension and slow down the liquid drainage speed in the film, increasing the foam life; this improves the foaming ability and foam stability [21,22].

Foam flow in porous media is a special gas–liquid two-phase flow; it is a process of migration, rupture, and regeneration of a series of liquid films. The tensile and compressive deformation of a liquid film through the throat is related to the flow resistance of foam in porous media. During the foam injection, the capillary force changes due to the difference in the concentration of foaming agent. When the concentration of foaming agent increases, the performance of generated foam becomes better, and the flow area of foam increases. Accordingly, the flow resistance of fluid in the pore increases. Thus, the subsequent fluid is diverted into the region not swept by the original injected water [23–27], and the resistance of foam makes the gas flow into smaller pores.

Extensive studies have been carried out on foam blocking capability. The effects of injection mode, injection rate, injection velocity, temperature, permeability, and optimization of foaming agent on foam blocking capability have been evaluated in detail, and the research on micromechanism of foam profile control and flooding has become more mature [28–35]. However, the changes in flow characteristics of foam with surfactant concentration during the foam transport in the formation have been rarely studied. When the foam flows in the formation, the surfactant is adsorbed on the surface of rock. This decreases the surfactant concentration and inevitably affects the properties and flow performance of foam in the formation. Therefore, it is essential to investigate the changes in foam performance along the flow direction caused by the change in surfactant concentration.

In this paper, core-flow experiments were performed to evaluate the flow characteristics of foam in porous media under different surfactant concentrations. A high-pressure visual unit was used to analyze the changes in foam texture. The relationship between foam texture and blocking capability under different surfactant concentrations was evaluated. Moreover, the effect of surfactant concentration on gas saturation in porous media was evaluated.

2. Experimental methods

2.1. Apparatus

The schematic of displacement apparatus used in this study is shown in Fig. 1. Sandpack models were used in the experiment; in all the experiments, the sandpacks were placed horizontally. Constant gas and liquid flow rates were applied, and the pressure differences in sandpacks were measured using pressure transducers (Model 3210PD, full-scale deflection of 20 MPa and accuracy of 0.1% full scale, Haian Group, China). The gas rate was regulated using a gas mass flow controller (Model 5850E, Brooks, USA) with a flow range of 0–50 mL/min (standard condition), pressure measurement range of 10.0 MPa, and an accuracy of 1% full scale. Fluid was delivered to the sandpack model at a preset constant volumetric flow rate using a pump (ISCO model 100 DX, with a flow accuracy of < 0.25 μL/min and pressure accuracy of < ± 0.5%). A foam generator packed with 70–100 μm silica sand was placed in the upstream of sandpack model. Foam was generated by injecting gas and surfactant solution to the foam generator. A high-pressure visual unit and a high-precision camera were used to record the changes in foam texture. A back-pressure regulator (BPR) with an open error of less than 0.001 MPa was used to control the back pressure. The change in the quality of sandpack was measured using a balance (Model PL2002, Mettler Toledo, Switzerland, full scale of 2100 g, accuracy of 0.01 g).

2.2. Materials

2.2.1. Sandpack

Silica sands of diverse size distributions were packed into a stainless-steel tube as a model of reservoir. The length of sandpack was 300 mm, and the internal diameter was 25 mm. The sand grains used in this experiment were of 120 mesh. The porosities and permeabilities were measured by brine flooding. The sandpacks used in the experiments almost had the same permeability ($875 \pm 20 \times 10^{-3}$ μm^2) and porosity (35.4 ± 0.20%).

2.2.2. Surfactant

SDS was used to perform foam experiments (purchased from Sigma, USA, with a purity of > 99.0%).

2.2.3. Brine

Analytically pure $CaCl_2$ and NaCl at concentrations of 1000 mg/L and 10,000 mg/L were used in the experiments to simulate formation water. $CaCl_2$ and NaCl were supplied by Sigma (USA), both with purity > 99.5%. Deionized water was used in the experiments; it was obtained by passing water through an ion exchanger. The density and viscosity of brine at 25 ℃ were 1016 kg/m^3 and 1.10 mPa·s, respectively.

2.2.4. Gas

Industrial-grade nitrogen gas with a purity of 99.99% was used in the experiments.

2.3. Experimental procedures

SDS solutions of different concentrations (0.001, 0.005, 0.10, 0.20, 0.30, and 0.50 wt%) were injected into a single-tube sandpack model from low to high concentration. The sandpack was saturated with water after vacuuming. Then, the pore volume was measured by weighing, and the permeability was obtained by measuring the pressure difference ΔP_1 of brine water flooding. Next, a pad fluid of surfactant solution was first injected into the model for 0.30 PV (pore volume, total volume occupied by the pores within the sandpack) at the injection rate of 1.0 mL/min, and the initial weight of the sandpack was measured. Then, foam was injected. During the injection, the injection rates of surfactant solution and gas were both 1.0 mL/min, and the pressure difference was measured in a certain time interval. After the pressure became stable, the weight of sandpack and the pressure difference ΔP_2 were measured again, and the foam in the visualization unit was observed and photographed. Finally, the simulated formation water was injected into the entire system for cleaning, and the weight of sandpack was recorded.

The experiments were continued by changing the surfactant concentration from small concentration to large concentration and repeating the above experimental steps. The resistance factor of foam was calculated using the following equation:

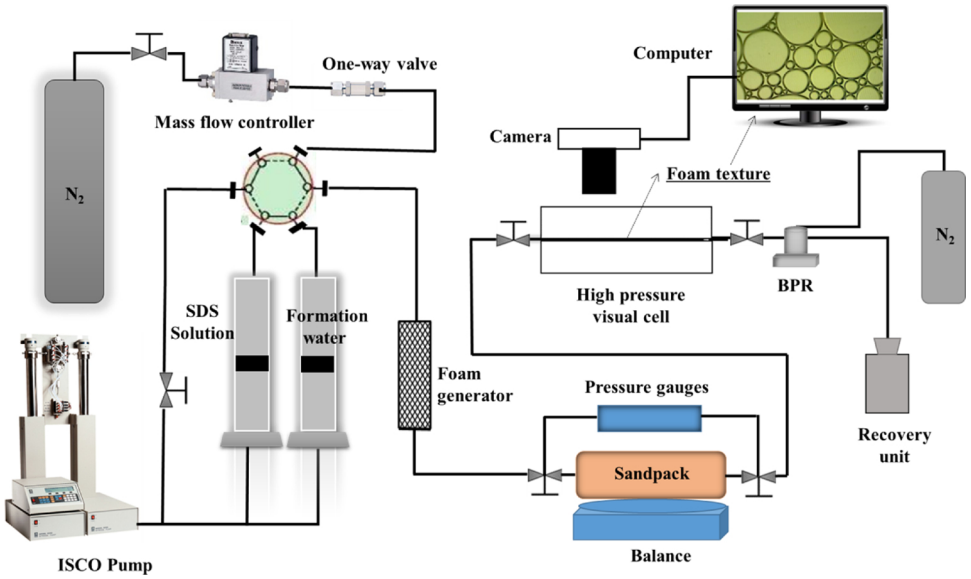

Fig. 1. Schematic diagram of core-flow experimental apparatus.

$$RF = \frac{\Delta P_2}{\Delta P_1}$$

where ΔP_1 is the pressure difference of water flooding between the inlet and outlet of sandpack under a given flow rate, MPa; ΔP_2 is the pressure difference of foam flooding between the inlet and outlet of sandpack under the same flow rate, MPa.

3. Experimental results and discussion

3.1. Analysis of foam texture and blocking capability

3.1.1. Foam blocking capability

The foaming agent with different surfactant concentrations was evaluated. The foaming volume and half-life of foam at different concentrations were measured by the Waring blender method [36]. The foaming capacity of foaming agent was expressed by the foam volume, and the foam stability was expressed by the half-life of foam. The results are shown in Fig. 2. With the increase in surfactant concentration, the foaming volume of foaming agent clearly increased, the half-life of foam prolonged, and the foaming capacity and foam stability increased. With the increase in the concentration of foaming agent, the growth rate of bubble volume and half-life slightly decreased.

Fig. 3 shows the pressure difference curve between the inlet and outlet of sandpack measured at different surfactant concentrations. When the pressure difference is stable, the blocking pressure and volume of foam injection are shown in Table 1, and the change in resistance factor is shown in Fig. 4.

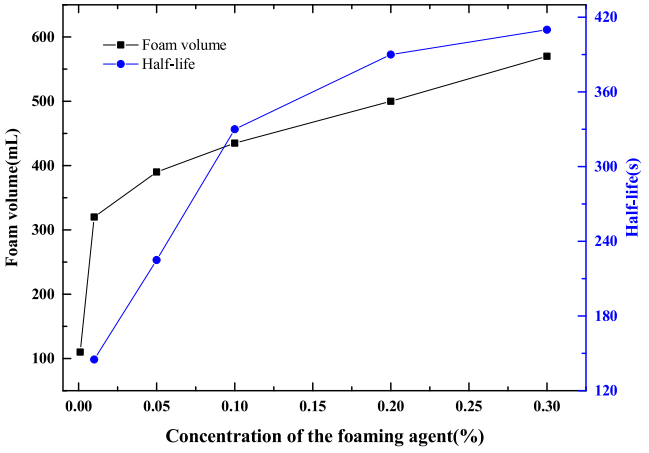

Fig. 2. Half-life time and foam volume at different concentrations.

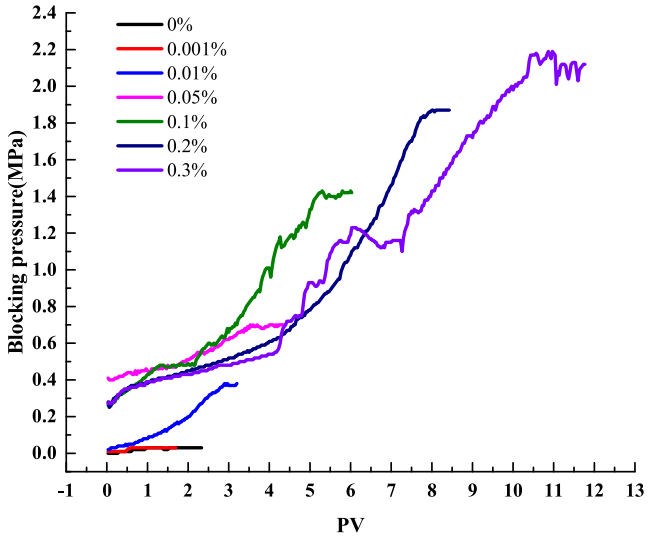

Fig. 3. Blocking pressure of foam at different surfactant concentrations.

Table 1
Injection volume of foam at different surfactant concentrations.

Surfactant concentration	Gas/liquid ratio	Blocking pressure (MPa)	Injection volume (gas breakthrough) (PV)	Injection volume (stable) (PV)
0%	1:1	0.03	0.10	1
0.001	1:1	0.03	0.10	1
0.01	1:1	0.38	0.15	3
0.05	1:1	0.70	0.17	3.5
0.1	1:1	1.42	0.25	5
0.2	1:1	1.87	0.25	8.1
0.3	1:1	2.12	0.30	11.8

In Table 1, gas breakthrough refers to the beginning of gas production at the outlet of the sandpack. By observing, when the small bubbles appear in the high temperature visualization unit, we will

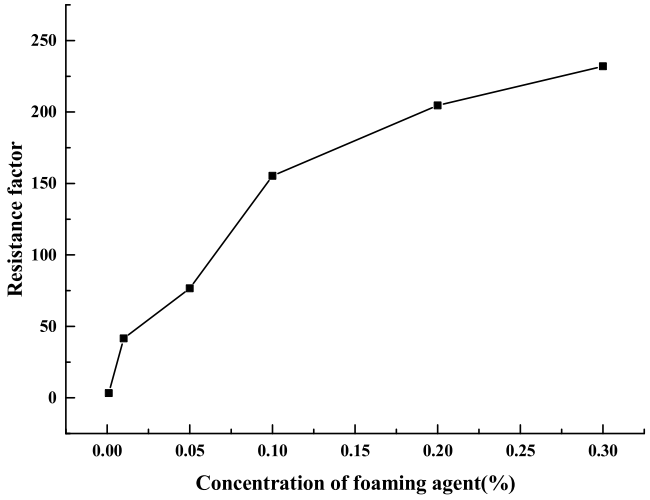

Fig. 4. Resistance factor at different concentrations of foaming agent.

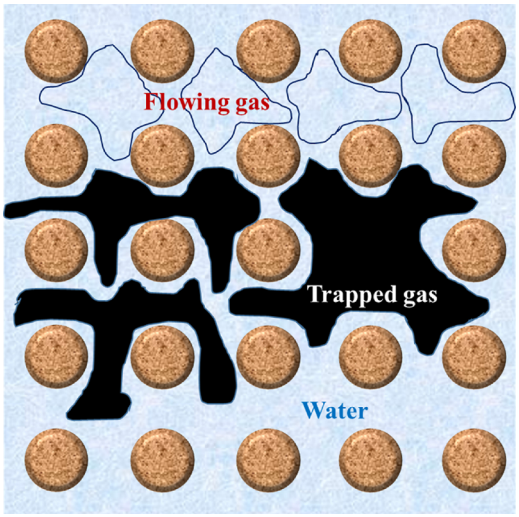

Fig. 5. Sketch map of distribution of foam in porous media.

record this time and calculate the injection volume before this time.

By observing and comparing the above results, it was found that (a) the foam blocking pressure fluctuation increases with the increase in foam injection volume and eventually reaches a stable state. As shown in Fig. 3, when the concentration of foaming agent is below 0.001%, the pressure difference between the inlet and outlet of sandpack during the foam injection does not clearly increase. When the concentration of foaming agent was increased to 0.01%, the pressure difference between the inlet and outlet of sandpack increased. With the increase in the concentration of foaming agent, the pressure difference between the inlet and outlet of sandpack increased. As shown in Fig. 4, the resistance factor rapidly increased with the increase in concentration. When the concentration was increased to ~0.1%, the increase in resistance factor started to decrease, and the resistance factor increased to 231.9 when the concentration of foaming agent was increased to 0.3%, which is 5.6 times the concentration of 0.01%. The blocking capability clearly improved; (b) As shown in Table 1, The lower the surfactant concentration, the faster the appearance of gas breakthrough. When the concentration of foaming agent was 0.001%, gas breakthrough appeared after the injection of 0.1 PV foam fluid. In other words, the foam injection volume increased with the increase in surfactant concentration when the gas breakthrough appeared. (c) The injection volume required for the pressure difference to reach stability increased with the increase in the concentration of foaming agent. When the concentration was 0.01%, the pressure was stabilized by the injection of ~3 P V foam. However, when the pressure was increased to 0.3%, the foam injection volume increased to 10 PV when the pressure was stable.

3.1.2. Foam texture

When foam is transported in porous media, because of the difference between the sizes of bubble and pore throat, the Jamin effect (resistance to liquid flow through capillaries which is due to the presence of bubbles) occurs in the pore throat due to the change in diameter, and the superposition of Jamin effect makes the foam to have the blocking pressure. It is generally believed that the gas and liquid of a foam flow separately in porous media. Gas-phase tracer experiments and CT studies show that the wetting water phase is mainly concentrated in the small pores, and the foam transport in larger pores occurs in the form of a bubble chain [37–39]. The foam distribution [40] is shown in Fig. 5. When the pressure gradient exceeds the threshold, the trapped gases in porous media flow again, resulting in a fluctuating growth of blocking pressure. When the foam of main flow channel flows in a bubble chain, the continuous bubbles produce capillary force due to the change in pore throat diameter. The capillary force is shown as resistance due to the difference in the radius of pore and throat.

The change in foam transport in porous media with different surfactant concentrations was photographed, and the variation in the distribution pattern with concentration was analyzed.

1) Foam texture at extremely low surfactant concentration

First, a mixed injection experiment of nitrogen and water without surfactant was carried out; then, an injection experiment of SDS foaming agent solution with a concentration of 0.01% was carried out.

The experimental results show that the blocking effect of foam with extremely low surfactant concentration was almost equal to that of pure water, and the calculated resistance factor was only 3.28. During the pure water experiment, a large amount of gas appeared when the injection volume was very low. As shown in Fig. 6, when the pressure was stable, the continuity of outflow gas was very strong. The large bubbles had no fixed shape during the flow with stronger deformability. When large bubbles encountered each other, they immediately coalesced into larger bubbles and had no stable form. The variation in fluid in the outlet can be observed by the visual element. It was found that when the concentration was 0.001%, compared with the pure water/gas experiment, the continuity of flow gas was weakened, and the bubbles became smaller and more dispersed. However, the shape of bubbles was still irregular and easy to be deformed during the flow.

2) Foam texture at low surfactant concentration

The experiments were continued by increasing the surfactant concentration and setting the concentration as 0.01% and 0.05%. After the pressure became stable, the foam in glass plate was photographed. Fig. 7 shows the foam images recorded using a microscope with 60-fold magnification. When the concentration was increased to 0.01%, the foam had a good shape with a regular circle, and gas was more clear as a dispersed phase. However, the contact between foams was not close, and the size distribution of foam was not uniform. Moreover, the coexistence of gas and foam was observed in the outlet, and the gas breakthrough decreased. The measurement software was used to calculate the frequency distribution and cumulative frequency distribution of foam diameter. As shown in Fig. 8(a), the size of foam diameter is different. The diameter distribution has no obvious concentration but is distributed in the range of 10–400 μm. The frequency distribution of foam in different diameter ranges fluctuated within 0–10%, and the

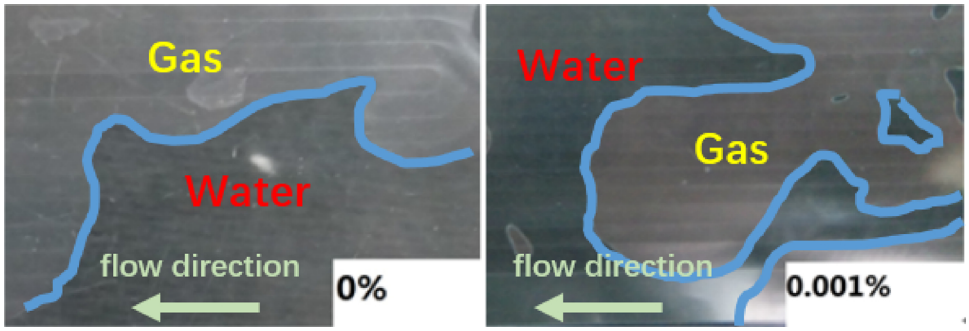

Fig. 6. Foam texture at extremely low surfactant concentrations (0% and 0.001%).

cumulative frequency distribution curve of foam was close to a straight line.

Compared with the 0.01% foam concentration, when the concentration of foaming agent was increased to 0.05%, the contact area between foams increased, and the bubbles were arranged closely. No obvious coalescence occurred when the bubbles encountered each other. The bubble has a thick film on the surface. On the macroscopic view, the diameter of foam clearly decreased. A relatively uniform foam was observed in the outlet, and the slug volume of gas was clearly controlled. According to the frequency distribution diagram of foam diameter (Fig. 8b), the diameter of foam generated under 0.05% concentration was distributed within 0–100 μm, but the diameter of foam was the largest in 5–10 μm, accounting for ~20% of the total. Thus, only 0.8% of bubble diameter is 95–100 μm. The cumulative frequency distribution curve of foam diameter was a convex curve. This strongly increased when the diameter was less than 50 μm, and the bubbles in the 0–50 μm range accounted for 80% of the total.

3) Foam texture at high surfactant concentrations

The surfactant concentration was set to a high concentration of 0.1%, 0.2%, and 0.3%. The foam status in a glass plate is shown as Fig. 9. The frequency distribution and cumulative frequency distribution curve are shown in Fig. 10. The foam was more closely arranged at a high concentration, and the degree of contact between bubbles was higher without obvious coalescence. When the concentration was increased from 0.1% to 0.3%, Fig. 9 shows that the diameter of bubbles decreased, and they became more concentrated. A uniform and milky white foam was found in the outlet. Better yet, the gas slug disappeared, and the gas breakthrough was effectively controlled.

The frequency distribution diagram of foam diameter at three concentrations is shown in Fig. 10. The diameter distribution in 5–10 μm clearly increased with the increase in foaming agent concentration. When the concentration of foaming agent was 0.1%, the bubbles of 5–10 μm accounted for ~32% of the total, slightly lower than 34% of the 0.2% concentration, and the frequency distribution reached 47% when the concentration was increased to 0.3%. However, more notably, the bubbles of 0–5 μm increased from 10% under 0.1% concentration to 34% under 0.3% concentration. In other words, more and more bubbles gathered to form bubbles with a smaller diameter, and the foam diameter distribution became more and more concentrated. The cumulative frequency distribution curve of foam diameter at three concentrations is still a convex curve, and the rising degree of curve in the first half increased with the increase in foaming agent concentration. When the concentration was 0.3%, the cumulative frequency distribution of foam in 0–15 um was up to 96%, slightly higher than 93% under 0.2% concentration, higher than 80% under 0.1% concentration, and the diameter of foam gradually concentrated to less than 10 μm with the increase in concentration.

4) Relationship between foam texture and surfactant concentration

The median diameter of foam and the diameter of maximum distribution frequency clearly show the distribution of foam diameter and degree of concentration of diameter. As shown in Fig. 11, the median diameter of foam gradually decreased with the increase in the concentration of foaming agent. When the concentration was increased to 0.1%, the median diameter of foam decreased from 60 μm to ~10 μm. The median diameter of foam was stable in the range of 5–10 μm with increasing concentration. The diameter of maximum distribution frequency also tends to smaller. When the concentration was 0.01%, the foam diameter was more distributed around 120 μm. When the concentration reached 0.3%, the maximum distribution frequency of bubble was concentrated to 5–10 μm.

Fig. 12 shows the variation curve of standard deviation of foam diameter with the change in concentration, reflecting the uniformity of foam. With the increase in concentration, the standard deviation of foam diameter decreased, indicating that the foam became more uniform and the individual difference between bubbles became smaller.

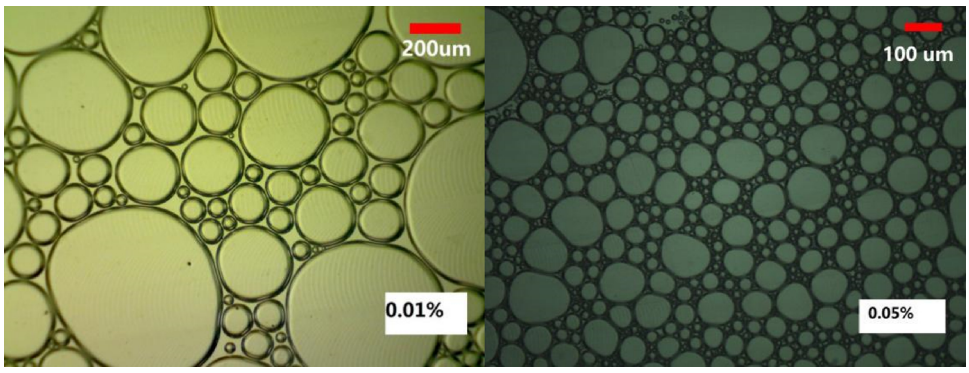

Fig. 7. Foam texture at low surfactant concentrations (0.01% and 0.05%).

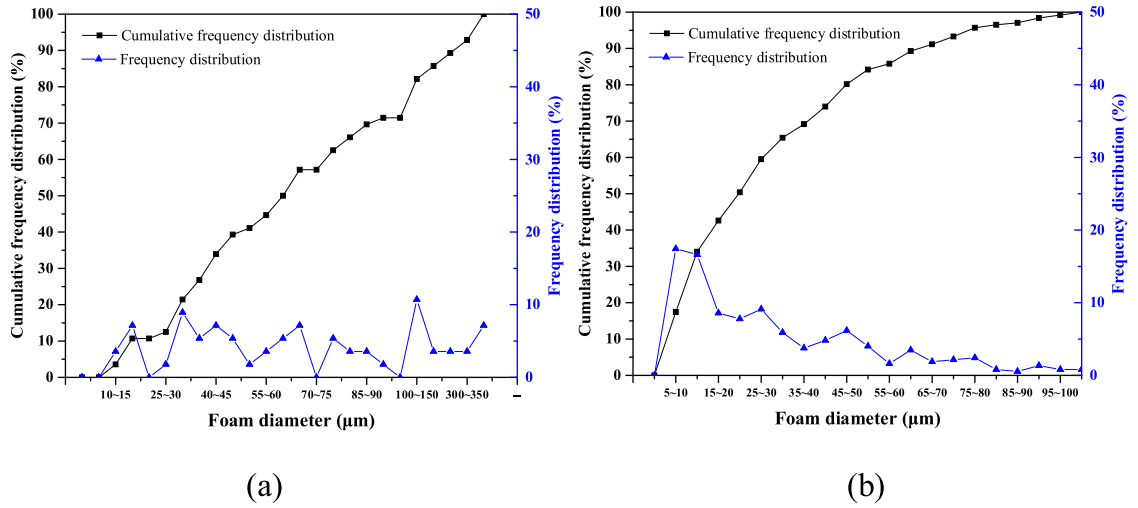

Fig. 8. Frequency distribution and cumulative frequency distribution of foam diameter at low surfactant concentrations (a, 0.01%; b, 0.05%).

3.2. Analysis of foam diameter and pore size

With the increase in surfactant concentration, the morphology of foam also changed. There is an inevitable relationship between the change in foam texture and pore structure. In this paper, the change in foam observed using a high-pressure visual device was used to indirectly determine the flow trend of foam in sandpack.

The pore structure of sandstone is very complex. To study the physical property of reservoir, a theoretical rock model was established to derive the quantitative relationship between porosity, permeability, and rock physical properties.

Based on the capillary bundle model, the relationship between the permeability of rock and average pore radius derived from the Poiseuille's formula and Darcy's Law can be established. The average pore diameter of core used in this experiment was calculated using the following formula:

$$d = 2\sqrt{\frac{8K}{\varphi}} \quad (1)$$

where d is the average pore radius, Φ is the porosity, and K is the permeability. The permeability and porosity of sandpack used in the experiment were 875.37×10^{-3} um^2 and 35.4%, respectively. Therefore, the average pore radius was 8.9 μm as calculated using formula (1).

The contrast in foam diameter obtained using the high-pressure visual unit in the range 0.01–0.3% was compared with Fig. 13. As shown in Fig. 13, a certain relationship exists between the diameter of foam and average pore diameter as the surfactant concentration increases. The smallest bubble diameter at 0.01% concentration was within 10 μm, and the maximum could reach 100 μm. The frequency distribution is a wavy curve. The numerical difference between bubble diameter and average pore diameter is very large; even the frequency distribution of foam diameter near 8.9 μm is only 2%. Thus, the matching degree of average pore diameter of core is very low. When the concentration was increased to 0.05%, the curve of frequency distribution began to protrude in the smaller diameter range, and the frequency distribution of foam diameter near 8.9 μm increased to 17%. When the concentration was 0.1–0.3%, the protruding of curve is more obvious, the frequency distribution of foam diameter greater than 50 μm is very small, and the diameter of most foams is within 50 μm. When the concentration was 0.3%, the protruding of curve was most obvious, and the frequency distribution of foam diameter was up to 47% at the core average pore diameter. The matching degree was much higher than that of foam generated by other concentration.

Weighted average method was used to calculate the average diameter of foam with the frequency distribution of foam diameter as the weight; the trend of average diameter of foam can be obtained at different concentrations of foaming agent (because good foam was not generated, the concentrations of 0.001% and 0.01% were not calculated).

As shown in Table 2, when the concentration is 0.05%, the average diameter of foam was 19.6 μm, very different from the average pore diameter of core (8.9 μm). When the concentration was increased to 0.1%, the average diameter of foam clearly decreased to 12.6 μm. The higher the concentration, the smaller the average diameter of foam, and the smaller the difference between the average diameter of foam and average pore diameter of core.

3.3. Analysis of surface tension and gas saturation

Interfacial tension can be used to determine the existence state of foam. The interfacial tension of a gas–liquid interface under different surfactant concentrations was measured using a TECLIS interfacial tension tester and our data approximately agreed with the previous

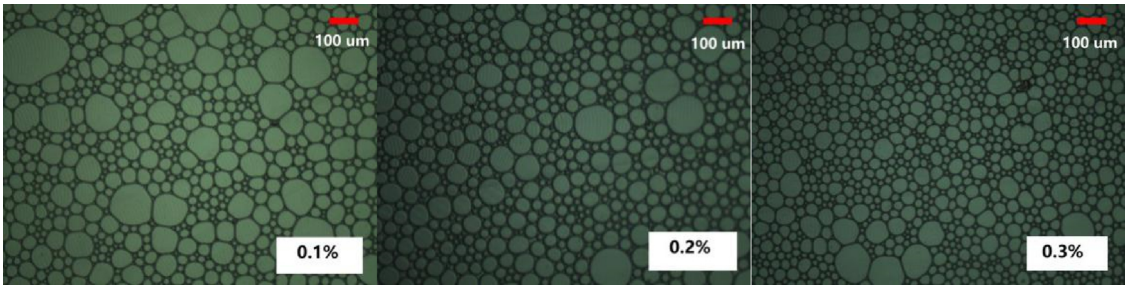

Fig. 9. Foam texture at high surfactant concentrations (0.1%, 0.2%, and 0.3%).

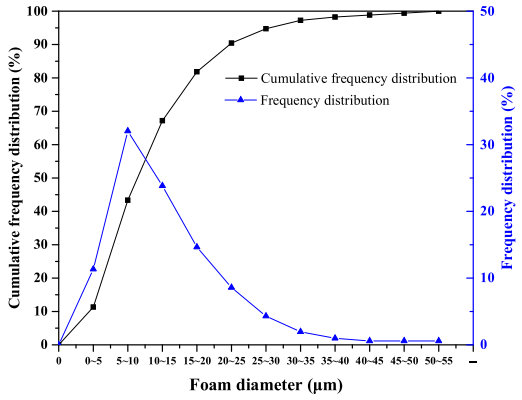

(a)

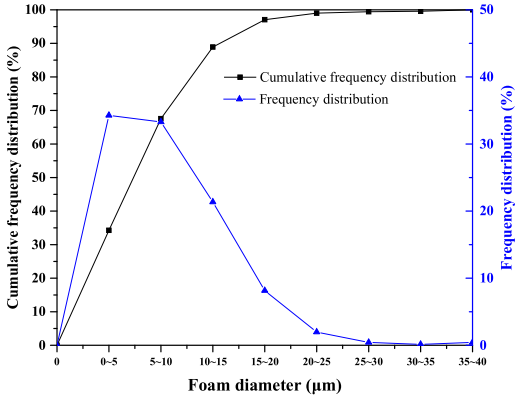

(b)

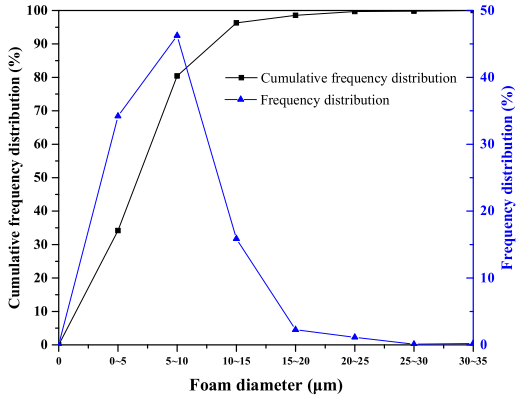

(c)

Fig. 10. Frequency distribution and cumulative frequency distribution of foam diameter at high surfactant concentrations (a, 0.01%; b, 0.05%; c, 0.3%).

results [41,42]. As shown in Fig. 14, the interfacial tension was higher when the surfactant concentration was lower, and the interfacial tension gradually decreased with the increase in surfactant concentration with the rate of decrease slowing down, and the CMC (critical micelle concentration) of SDS is 0.23%. The higher interfacial tension does not increase the stability of foam. Therefore, the generated foam will easily rupture, and the gas cannot be controlled during the flow. The lower interfacial tension decreases the energy of foam system, which is beneficial for the stability of the foam. The generated foam is not easy to rupture during the flow in the formation, and the gas breakthrough can be controlled.

When a foam fluid flows in the core, if more than 80% of gas is trapped, the trapped foam will severely decrease the effective permeability of gas in porous media, thus increasing the flow resistance. In the

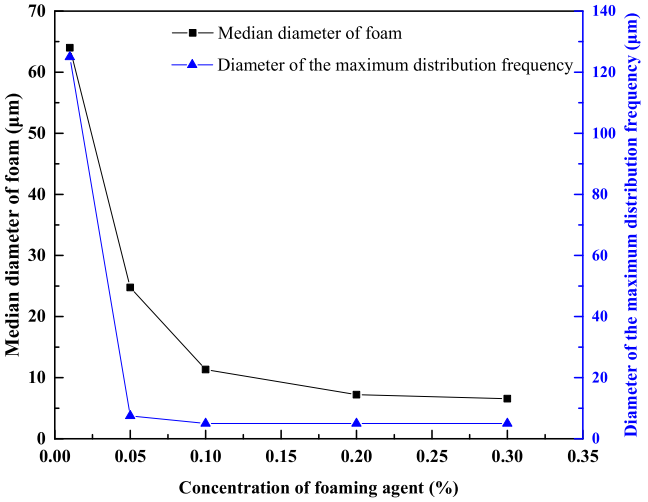

Fig. 11. Median diameter of foam and diameter of maximum distribution frequency at different surfactant concentrations.

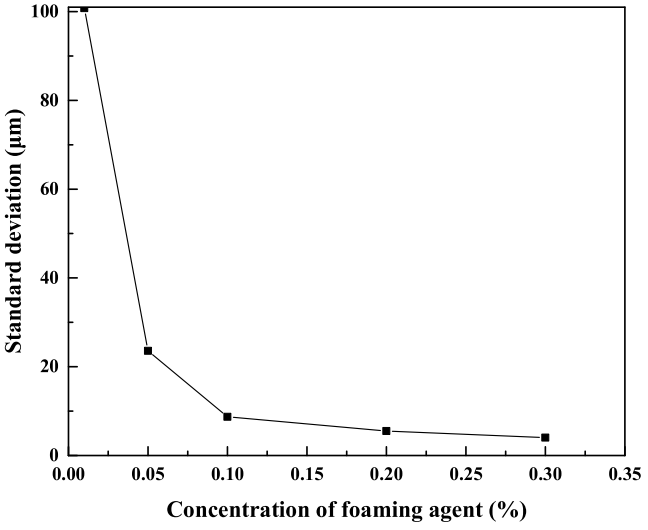

Fig. 12. Standard deviation of foam diameter at different surfactant concentrations.

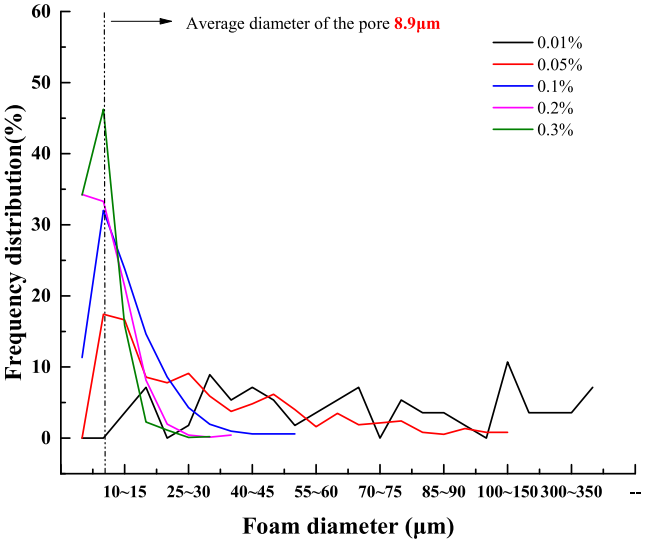

Fig. 13. Frequency distribution at different surfactant concentrations.

Table 2
Average foam diameter at different surfactant concentrations.

Surfactant concentration (%)	Average pore diameter (μm)	Average foam diameter (μm)
0.05	8.9	19.6
0.1	8.9	12.6
0.2	8.9	9.4
0.3	8.9	7.9

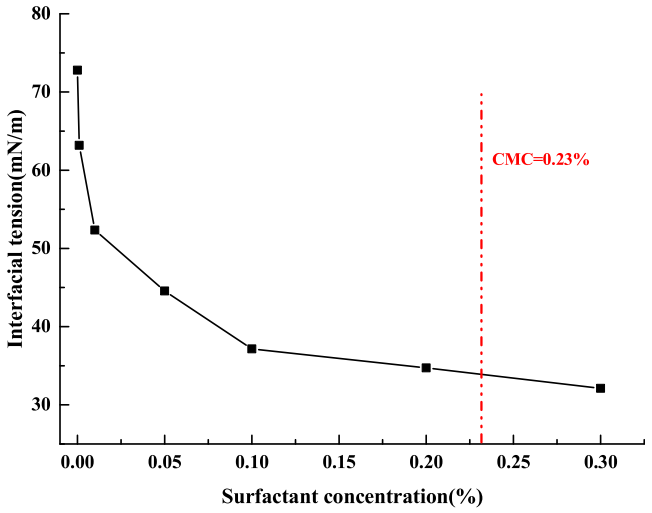

Fig. 14. Variation in interfacial tension with the change in surfactant concentration.

presence of foam, the number of pore channels used for gas transfer is 100 times smaller than that of fluid without foam [43–45]. During the foam displacement, the gas saturation of core is related to the blocking capability of foam. Effective blocking can be achieved only when the gas saturation reaches more than 60% in the core, making the resistance factor increase rapidly. During the porous flow, the change in gas saturation can directly reflect the volume of trapped gas in the core. With the increase in the pressure of foam blocking, more and more gases were diverted into small pores.

After measuring the wet weight of core saturated water and the change in core weight during the foam flow in porous media, the change in gas saturation in the core can be obtained by calculating the weight difference by neglecting the gas weight. Notably, parameters such as the injection velocity of gas and liquid cannot be changed during the experiment.

The change in gas saturation in the core with the concentration of foaming agent is shown in Fig. 15. When the surfactant concentration was low, the gas saturation was low, and the volume of gas occupying the pores was small. Thus, the volume of trapped gas was small. When the concentration was increased to 0.1%, the gas saturation reached 70%, and the volume of gas occupying pores increased. With the continuous increase in concentration, the gas saturation became stable and eventually reached 84.5%, and a large amount of gas was trapped in the core.

The interfacial tension of foaming agent solution and nitrogen is closely related to gas saturation in the core. The addition of a surfactant can effectively decrease the interfacial tension of gas and water, thus enhancing the stability of foam. When foam transport occurred in the formation, more and more space was occupied by the foam due to the Jamin effect and blocking capacity, and the gas was diverted into smaller pores and trapped. Therefore, the gas breakthrough was controlled effectively, and the swept volume of foam fluid increased.

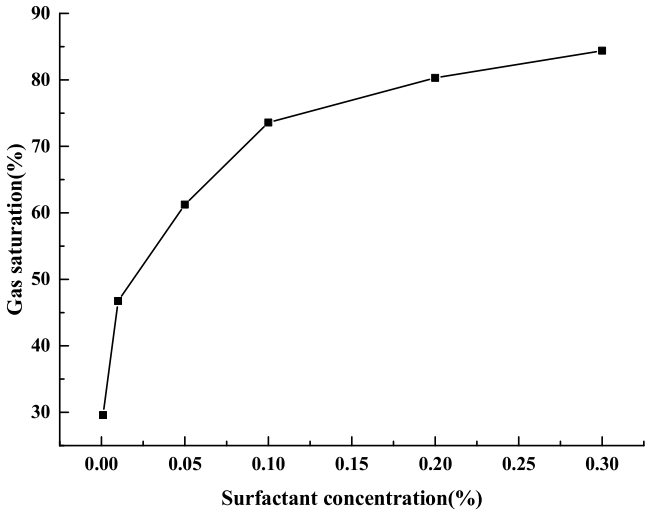

Fig. 15. Variation in gas saturation with the change in surfactant concentration.

4. Conclusions

(1) With the increase in the concentration of foaming agent, the surface tension of gas and liquid decreases, the foam stability increases, the flow resistance in the core increases, and a longer time is taken by the foam flow to reach stability. When the concentration of foaming agent reaches the critical value, the reduction amplitude of surface tension decreases, and the rate of increase of foam flow resistance slows down.

(2) A stable foam cannot be formed at an extremely low concentration of foaming agent, and the flow in porous media is close to pure gas–liquid two-phase flow. With the increase in the concentration of foaming agent, the stability of foam is enhanced. The average diameter of bubbles in the porous media decreases, the bubble is more uniform, and the foam is arranged closely.

(3) The blocking capability of foam in porous media is closely related to foam texture. The smaller the average diameter of the bubbles, the more uniform the distribution, and the stronger the blocking capability of foam. With the increase in the concentration of foaming agent, the average diameter of bubble decreases, and the matching degree with average pore diameter increases. The maximum distribution frequency of bubbles is consistent with the average pore diameter of core.

(4) With the increase in surfactant concentration, the stability of foam is enhanced, the proportion of trapped gas in porous media increases, the gas saturation in the core increases, and the flow resistance of foam increases. After the surfactant concentration reaches the critical value, the increase amplitude of gas saturation became smaller, and the gas saturation was more than 80% when the foam quality was 50%.

Acknowledgements

This work was financially supported by the National Science and Technology Major Project of the Ministry of Science and Technology of China (No. 2016ZX05056-001), Postdoctoral Researcher Applied Research Project Funding of Qingdao, China (040000639) and the Project funded by China Postdoctoral Science Foundation (2018M632637) and the National Natural Science Foundation of China (No. 51574264). We sincerely thank other persons in the Foam Research Center in China University of Petroleum (East China) and Geo-Energy Research Institute for helping with the experimental research.

References

[1] J.X. Wang, L. Han, L.I. Song-Yan, T.F. Wang, Application status and prospect of foam fluid in oil field, Appl. Chem. Ind. 41 (8) (2012) 1408–1411.
[2] F. Friedmann, W.H. Chen, P.A. Gauglitz, Experimental and simulation study of high-temperature foam displacement in porous media, SPE Reservoir Eng. 6 (1) (1991) 37–45.
[3] G.G. Bernard, L.W. Holm, Effect of foam on permeability of porous media to gas, Soc. Pet. Eng. J. 4 (3) (1964) 267–274.
[4] R.A. Albrecht, S.S. Marsden, Foams as blocking agents in porous media, Soc. Pet. Eng. J. 10 (1) (1970) 51–55.
[5] M. Kanda, R.S. Schechter, On the Mechanism of Foam Formation in Porous Media. Spe Fall Technical Conference and Exhibition. Society of Petroleum Engineers, (1976).
[6] F. Friedmann, J.A. Jensen, Some parameters influencing the formation and propagation of foams in porous media, Acta Ophthalmol. (Copenh.) 56 (6) (1986) 977–983.
[7] A.R. Kovscek, Q. Chen, M. Gerritsen, Modeling foam displacement with the local-equilibrium approximation: theory and experimental verification, SPE J. 15 (1) (2010) 171–183.
[8] Q.P. Nguyen, P.L.J. Zitha, P.K. Currie, W.R. Rossen, CT study of liquid diversion with foam, Spe Prod. Oper. 24 (1) (2005) 12–21.
[9] S.M. Hosseininasab, P.L.J. Zitha, Investigation of chemical-foam design as a novel approachtoward immiscible foam flooding for enhanced oil recovery, Energy Fuels 31 (10) (2017) 10525–10534.
[10] Q.P. Nguyen, Systematic study of foam for improving sweep efficiency in chemical enhanced oil recovery, Surgery 142 (1) (2011) 20–25.
[11] R. Farajzadeh, A. Andrianov, R. Krastev, G.J. Hirasaki, W.R. Rossen, Foam-oil interaction in porous media: implications for foam assisted enhanced oil recovery, Adv. Colloid Interface Sci. 183–184 (2012) 1–13.
[12] R. Farajzadeh, A. Andrianov, P.L.J. Zitha, Investigation of immiscible and miscible foam for enhancing oil recovery, Ind. Eng. Chem. Res. 49 (4) (2010) 1910–1919.
[13] A.T. Turta, A.K. Singhal, Field foam applications in enhanced oil recovery projects: screening and design aspects, J. Can. Pet. Technol. 41 (10) (2002).
[14] PaulBecher, A review of: âfoams: fundamentals and applications in the petroleum industryiâ, l. e. schramm, ed. (advances in chemistry 242), American chemical society, Washington, d.c. 1994, pp xii + 555, $129.95 (issn 0065-2393; 242), J. Dispers. Sci. Technol. 17 (4) (1996) 451-451.
[15] S.A. Farzaneh, M. Sohrabi, A Review of the Status of Foam Application in Enhanced Oil Recovery, (2013).
[16] L.W. Lake, Enhanced oil recovery, Enhanced Oil Recov. 59 (10) (1989) 839A–852A.
[17] R.D. Gdanski, Experience and research show best designs for foam-diverted acidizing, Oil Gas J. 91 (36) (1993) 85–89 36.
[18] L. Cheng, S.I. Kam, M. Delshad, W.R. Rossen, Simulation of dynamic foam-acid diversion processes, SPE J. 7 (3) (2002) 316–324.
[19] A.H. Falls, G.J. Hirasaki, T.W. Patzek, D.A. Gauglitz, D.D. Miller, T. Ratoulowski, Development of a mechanistic foam simulator: the population balance and generation by snap-off, SPE Reservoir Eng. 3 (3) (1988) 884–892.
[20] A.R. Kovscek, Fundamentals of Foam Transport in Porous Media, (1994).
[21] S. Qian, Z. Li, S. Li, J. Lei, J. Wang, W. Peng, Utilization of surfactant-stabilized foam for enhanced oil recovery by adding nanoparticles, Energy Fuels 28 (4) (2014) 2384–2394.
[22] Q. Sun, Z. Li, J. Wang, S. Li, B. Li, L. Jiang, et al., Aqueous foam stabilized by partially hydrophobic nanoparticles in the presence of surfactant, Colloids Surf. A Physicochem. Eng. Aspects 471 (2015) 54–64.
[23] O. Pitois, C. Fritz, M. Vignes-Adler, Hydrodynamic resistance of a single foam channel, Colloids Surf. A Physicochem. Eng. Aspects 261 (1) (2012) 109–114.
[24] P.A. Gauglitz, F. Friedmann, S.I. Kam, W.R. Rossen, Foam generation in homogeneous porous media, Chem. Eng. Sci. 57 (19) (2002) 4037–4052.
[25] M. Chen, Y.C. Yortsos, W.R. Rossen, Insights on foam generation in porous media from pore-network studies, Colloids Surf. A Physicochem. Eng. Aspects 256 (2) (2005) 181–189.
[26] S.J. Neethling, H.T. Lee, P. Grassia, The growth, drainage and breakdown of foams, Colloids Surf. A Physicochem. Eng. Aspects 263 (1) (2005) 184–196.
[27] W.R. Rossen, M.W. Wang, Modeling foams for acid diversion, SPE J. 4 (2) (1997) 92–100.
[28] O.S. Owete, W.E. Brigham, Flow behavior of foam: a porous micromodel study, SPE Reservoir Eng. 2 (3) (1983) 315–323.
[29] P.A. Gauglitz, C.J. Radke, An experimental investigation of gas-bubble breakup in constricted square capillaries, J. Pet. Technol. 39 (9) (1987) 1137–1146.
[30] C.J. Radke, T.C. Ransohoff, Mechanism of foam generation in glass-bead packs, SPE Reservoir Eng. 3 (2) (1988) 573–585.
[31] P. Armitage, R.A. Dawe, What is the rheology of foam in porous media? A micromodel study, SPE International Symposium on Oilfield Chemistry, (1989).
[32] M.D.T. Pinto, M.A. Abraham, R.L. Cerro, How do bubbles enter a capillary? Chem. Eng. Sci. 52 (11) (1997) 1685–1700.
[33] K. Benkrid, S. Rode, M.N. Pons, P. Pitiot, N. Midoux, Bubble flow mechanisms in trickle beds—an experimental study using image processing, Chem. Eng. Sci. 57 (16) (2002) 3347–3358.
[34] J. Hou, Q. Du, Z. Li, G. Pan, X. Lu, K. Zhou, Experiments on foam texture under high pressure in porous media, Flow Meas. Instrum. 33 (10) (2013) 68–76.
[35] B. Géraud, S.A. Jones, I. Cantat, B. Dollet, Y. Méheust, The flow of a foam in a two-dimensional porous medium, Water Resour. Res. 52 (2) (2016) 773–790.
[36] M.M. Hashem, et al., Foaming agent, U. S Patent 7 (1985) 18 4524002.
[37] D. Du, P.L.J. Zitha, M.G.H. Uijttenhout, Carbon dioxide foam rheology in porous media: a ct scan study, SPE J. 12 (2) (2007) 245–252.
[38] M. Simjoo, Q.P. Nguyen, P.L.J. Zitha, Rheological transition during foam flow in porous media, Ind. Eng. Chem. Res. 51 (30) (2012) 10225–10231.
[39] Z. Li, William R. Rossen, Quoc P. Nguyen, Three-dimensional modeling of tracer experiments to determine gas trapping in foam in porous media, Energy Fuels 24 (5) (2007) 3239–3250.
[40] J.V. Gillis, C.J. Radke, A Dual Gas Tracer Technique for Determining Trapped Gas Saturation During Steady Foam Flow in Porous Media, (1990).
[41] I. Varga, R. Mészaros, T. Gilanyi, Adsorption of sodium alkyl sulfate homologues at the air/solution interface, J. Phys. Chem. B 111 (25) (2007) 7160–7168.
[42] Q. Sun, Z. Li, J. Wang, S. Li, B. Li, L. Jiang, et al., Aqueous foam stabilized by partially hydrophobic nanoparticles in the presence of surfactant, Colloids Surf. A Physicochem. Eng. Aspects 471 (2015) 54–64.
[43] R.W. Flumerfelt, H.L. Chen, W. Ruengphrathuengsuka, W.F. Hsu, J. Prieditis, Network analysis of capillary and trapping behavior of foams in porous media, SPE Form. Eval. 7 (1) (1992) 25–33.
[44] J. Prieditis, A Pore Level Investigation of Foam Flow Behavior in Porous Media, Univ. of Houston, Houston, TX (US), 1988.
[45] R.W. Flumerfelt, J.P. And, Mobility of Foam in Porous Media, (1988).